

# Plasma-sprayed cordierite: structure and transformations

H. G. WANG, G. S. FISCHMAN\*, H. HERMAN

*Department of Materials Science and Engineering, State University of New York at Stony Brook, Stony Brook, New York 11794-2275, USA*

Powdered cordierite (fused and mechanically reduced) feedstock was plasma-sprayed onto a steel substrate and subsequently removed. The substrate-free deposit was thermally cycled and investigated using differential thermal analysis, X-ray diffraction and transmission electron microscopy (TEM). The deposit as sprayed is amorphous, with crystallization to  $\mu$ -cordierite occurring at ca. 830°C, followed by a transition to high-cordierite at ca. 1000°C. The transition temperature is influenced by the heating rate and the geometry of the sample. Isothermal kinetic studies of crystallization were carried out, with the growth of the crystalline phase being described by a Johnson-Mehl-Avrami equation. The activation energies were obtained from the differential thermal analysis.

## 1. Introduction

Cordierite,  $2\text{MgO} \cdot 2\text{Al}_2\text{O}_3 \cdot 5\text{SiO}_2$ , is an oxide having a very low thermal expansivity and therefore good thermal shock resistance. The oxide is suitable for industrial applications, such as heat exchangers for gas turbine engines and as a catalyst carrier for automobile exhaust gas control [1-5]. Cordierite also possesses a low dielectric constant, high electrical resistivity and high chemical durability. As a result, this oxide has been used for integrated circuit substrates and insulators [6-7]. Bulk cordierite specimens can be fabricated by hot-pressing at  $200 \text{ kg cm}^{-2}$  in the temperature range from 950 to 1350°C [3]. Other fabrication methods, such as extrusion, have also been employed [8].

Phase decomposition studies were carried out on glassy cordierite which was formed by melting the material, > 1500°C and quenching in an aqueous solution [6, 9, 10]. On devitrifying the glass in the temperature range from 800 to 950°C, a metastable  $\mu$ -cordierite was obtained, which underwent a reconstructive phase transformation to a high-cordierite structure at  $\sim 1000^\circ\text{C}$ . The variation in the transition temperatures reported were mainly due to the differences in chemical composition and mass of the material [6, 9-14].

In the present study, we report on cordierite deposits which have been formed by plasma spraying. The phase structures and transition temperatures are examined following annealing. Isothermal crystallization is studied and a Johnson-Mehl-Avrami equation is thereby obtained. Activation energies for the phase transitions are evaluated from differential thermal analysis at different heating rates.

## 2. Experimental procedure

The material used in this investigation is a fused, cast, comminuted cordierite supplied by Muscle Shoals

TABLE I The chemistry of cordierite powder (wt %)

MgO <sub>2</sub>	17.89
Al <sub>2</sub> O <sub>3</sub>	31.20
SiO <sub>2</sub>	50.20
Other	0.71

Minerals, Tuscumbia, Alabama, USA. An SEM of the as-received particles is shown in Fig. 1 and the nominal oxide chemistry is given in Table I. The mean particle size is about 60  $\mu\text{m}$ . Using an automated plasma spray system (Plasma-Technik, Switzerland), the powder was deposited onto a NaCl-coated steel substrate. After spraying, the deposit was removed from the substrate by immersion in water, which dissolved the NaCl layer at the steel-ceramic coating interface. The plasma spray parameters are given in Table II.

For differential thermal analysis, DTA (Perkin-Elmer 1700), the pulverized deposit was compared to a powdered alumina reference for temperatures ranging continuously from room temperature to 1350°C. The samples were heated at various rates.

For crystallization studies, the sprayed deposits were annealed at 870°C as a function of time. The samples were then air-cooled and X-ray diffractometry was carried out using Cu-K $\alpha$  radiation at 35 kV and 15 mA. Two deposits were ion-beam thinned for TEM studies. One in the sprayed condition and another following annealing at 870°C for 8 h.

TABLE II The plasma-spray parameters

Primary gas; Ar (SLPM)	30
Secondary gas; H <sub>2</sub> (SLPM)	12
Carrier gas; Ar (SLPM)	3.4
Current (A)	450
Voltage (V)	74
Spray distance (mm)	125
Spray rate (g/min)	9

\* Present address: CES Division, New York State College Ceramics, Alfred University, Alfred, New York 14802-1296, USA



Figure 1 SEM of cordierite powder.

### 3. Results and discussion

Because of the very high cooling rate experienced by the plasma sprayed deposits ( $\sim 10^6$  deg/sec) and the presence of 50%  $\text{SiO}_2$ , sprayed cordierite is expected to be amorphous, as demonstrated by the X-ray diffraction plot in Fig. 2.

DTA results for a heating rate of  $40^\circ/\text{min}$  for a plasma-sprayed and pulverized cordierite sample is shown in Fig. 3. A small exothermic peak occurs at  $\sim 840^\circ\text{C}$ . Based on X-ray diffraction (Fig. 4), this thermal event is associated with a transition amorphous to  $\mu$ -cordierite, which has a crystal structure similar to that of  $\alpha$ -quartz [11]. A dominant (101) diffraction peak is very useful for examining the crystallization process. Mullite and high-cordierite are also detected in this pattern. On further heating (Fig. 3), an exothermic peak, with a maximum at  $1060^\circ\text{C}$  occurs in the temperature range of 980 to  $1120^\circ\text{C}$ . As noted from the diffraction plot of Fig. 5, this appears to be associated with the transition of  $\mu$ -cordierite to high-cordierite. Upon cooling from  $1350^\circ\text{C}$ , no peaks can be found in the DTA curve, suggesting that the  $\mu$ -cordierite is metastable.

These transition temperatures were noted to depend on the heating rate and the surface/volume ratio of the sample. As demonstrated for four heating rates (Fig. 6), an increase in heating rate will limit the time of the phase transformation and therefore increase the transition temperature. Furthermore, as shown in Fig. 7 for three sample sizes, the sample with a large particle size results in a reduction of the surface/

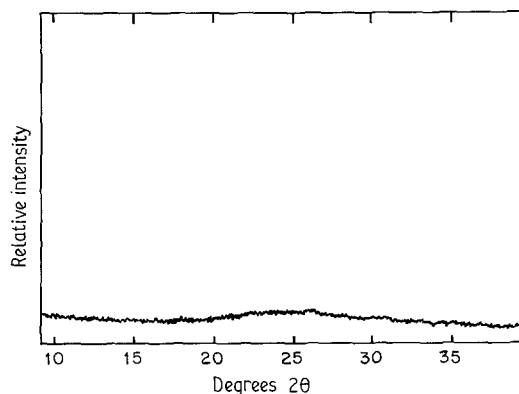


Figure 2 X-ray diffraction pattern of plasma-sprayed cordierite showing diffuse scattering resulting from amorphous structure.

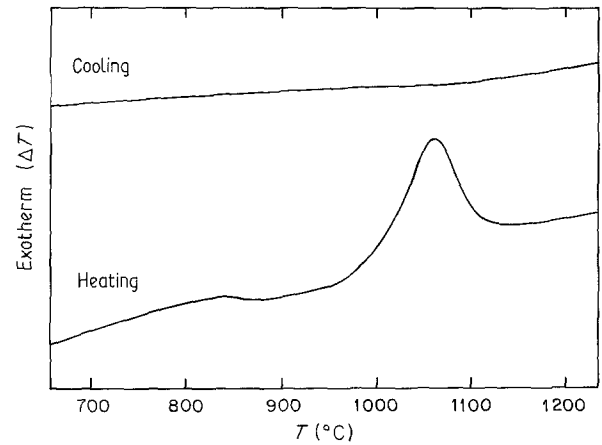


Figure 3 DTA curve of plasma-sprayed cordierite at a heating rate of  $40^\circ\text{C}/\text{min}$  showing transition temperatures.

volume ratio, hence, will increase the transition temperature.

Crystallization from an amorphous phase can be described by a Johnson-Mehl-Avrami Equation:

$$X = 1 - \exp(-kt^m) \quad (1)$$

if a straight line is found from  $\ln \ln (1/(1-X))$  against  $\ln(t)$  plot, where  $X$  is the vol % of crystalline phase,  $t$  is the annealing time,  $k$  is a kinetic constant and  $m$  is a morphology index [15].

The growth rate of the crystalline phase at  $870^\circ\text{C}$  was measured by the relative intensity of the (101) diffraction peak. The peak was normalized to the intensity of the (101) peak after long annealing times for which no further growth of crystalline phase could be detected using X-ray diffraction. From linear regression analyses of the data, the crystallization process at  $870^\circ\text{C}$  can be described by Equation 1 with  $k = 6.5 \times 10^4$  and  $m = 1.7$  (Figs 8a and b).

The morphology of the growing crystal was investigated by TEM; Fig. 9 is a micrograph of the ion-thinned sprayed deposit. The lack of contrast in the bright-field image and presence of diffuse halos in the selected diffraction pattern testify to the nature of amorphicity. Fig. 10 is a micrograph of an ion-thinned deposit annealed at  $870^\circ\text{C}$  for 8 h. The image shows phase separation with a spacing in the order of 5 to 6 nm. It should be noted that this spacing is consistent with what has been observed in  $\text{Al}_2\text{O}_3$ - $\text{SiO}_2$  glasses

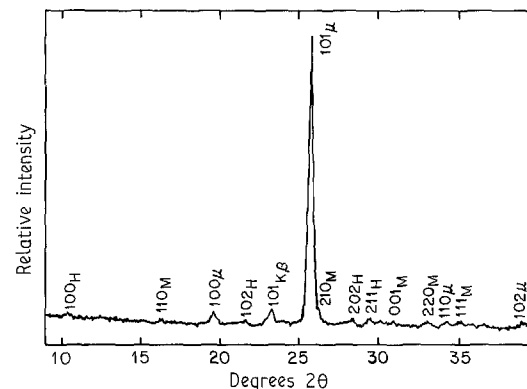


Figure 4 X-ray diffraction pattern of plasma-sprayed cordierite annealed at  $900^\circ\text{C}$  for 4 h. (M) Mullite; (H) High cordierite; ( $\mu$ )  $\mu$ -cordierite.

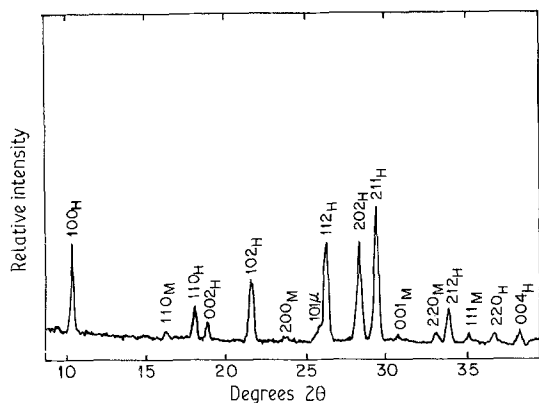


Figure 5 X-ray diffraction pattern of plasma-sprayed cordierite annealed at 1050°C for 2h. (M) Mullite; (H) High cordierite; ( $\mu$ )  $\mu$ -cordierite.

which undergo spinodal decomposition [16]. The evolution of a modulated structure indicates the occurrence of uphill diffusion and, implies that the amorphous sprayed cordierite is situated within a miscibility gap at 870°C. No supportive evidence exists that spinodal decomposition occurs in amorphous cordierite. This development of a composition instability occurs prior to the crystallization to  $\mu$ -cordierite. It must, of course, be recognized that the sprayed deposit is not chemically homogeneous and phase decomposition will not therefore be uniformly distributed. Figs 11 and 12 are in the same condition as Fig. 10, but were from different regions of the annealed deposit. The image of Fig. 11 shows that crystal growth occurs concurrently with the modulated structure and along the interface of the splatted particles; crystallization occurs within the particle as well. The spotty diffraction circles superimposed on the diffuse halos reveal  $\mu$ -cordierite which is emerging from the modulated amorphous structure. The image of Fig. 12 shows that crystallization can occur along a microcrack.

The activation energy of relevant phase transitions can be obtained from DTA measurements using the Kissinger Equation [17]:

$$\ln(\alpha/T_m^2) = -E/RT_m + \text{constant} \quad (2)$$

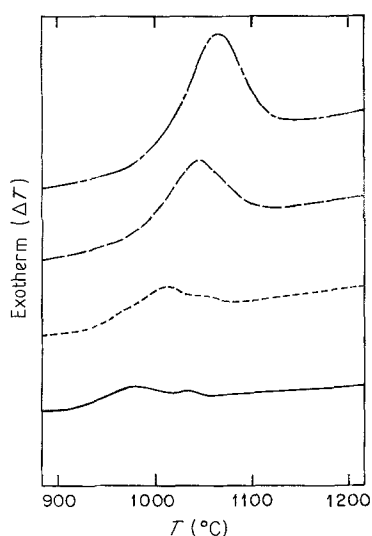


Figure 6 DTA curves of plasma-sprayed cordierite at four different heating rates for particle sizes  $< 63 \mu\text{m}$ . (—) 4°C min; (---) 10°C min; (-·-·-) 25°C min; (·-·-·) 40°C min.

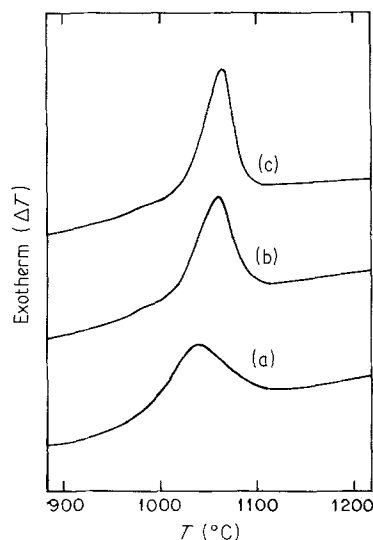


Figure 7 DTA curves of plasma-sprayed cordierite for three different sample sizes at a heating rate of 25°C/min. (a) Particle size  $< 63 \mu\text{m}$ ; (b) particle size between 590 and 840  $\mu\text{m}$ ; (c) coating size  $1 \times 2 \times 4 \text{mm}^3$ .

where  $\alpha$  is the heating rate,  $T_m$  is the temperature at which the maximum rate of conversion occurs and  $E$  is the activation energy. From the slope of the straight line in Fig. 13, the activation energy of phase transition from  $\mu$ -cordierite to high-cordierite is 400 kJ mol<sup>-1</sup>. As a reference, the activation energy of formation of high-cordierite from glass has been estimated to be 585 kJ mol<sup>-1</sup> from viscosity measurements and 272 kJ mol<sup>-1</sup> from DTA studies [6]. However, as suggested by Matusita *et al.* [18], the activation energy of crystallization should be determinable using a Kissinger-type Equation where the crystallization mechanism was considered. The activation energy for  $\mu$ -cordierite growth from amorphous phase has been

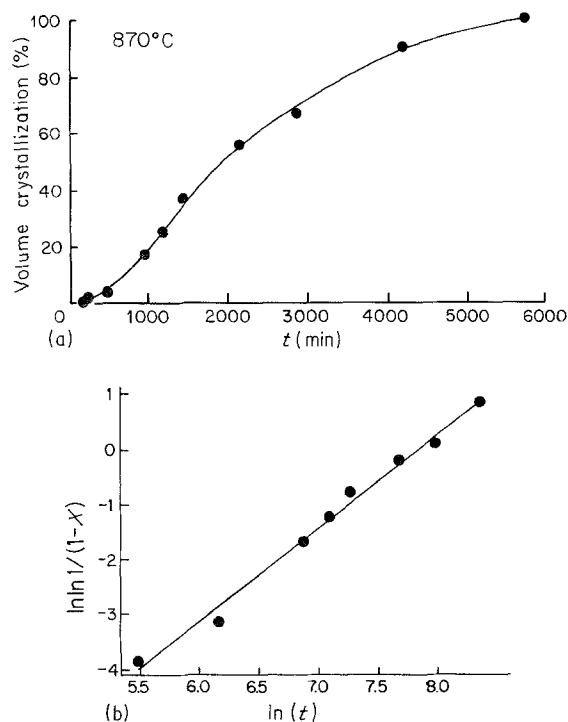


Figure 8 (a) Isothermal crystallization at 870°C; (b) Kinetic analysis of data of Fig. 8a using Equation 1.

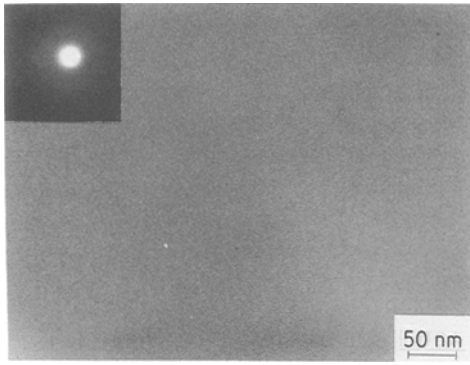


Figure 9 TEM micrograph of ion-thinned sprayed coating displaying amorphous structure.

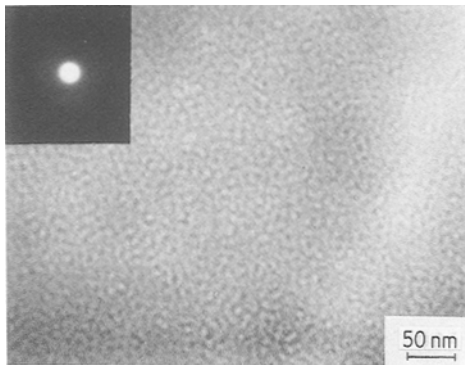


Figure 10 TEM micrograph of annealed deposit (870°C for 8 h) showing precrystallization phase separation.

estimated to be  $1600 \text{ kJ mol}^{-1}$  [19]. Therefore, long-time heating was required for devitrification of cordierite glass to  $\mu$ -form at 800 to 900°C [11].

By carrying out separate DTA studies of the cordierite and a standard sample of  $\text{ZrO}_2$ , an enthalpy change for the cordierite could be obtained, since the heat of formation of the monoclinic-to-tetragonal structure of  $\text{ZrO}_2$  is well known. The main contribution to the heat effect originates from the formation of high-cordierite, which is about 150 times greater than the heat of formation of  $\mu$ -cordierite. Therefore, the enthalpy change from the amorphous condition to high-cordierite is estimated to be  $240 \text{ kJ mol}^{-1}$

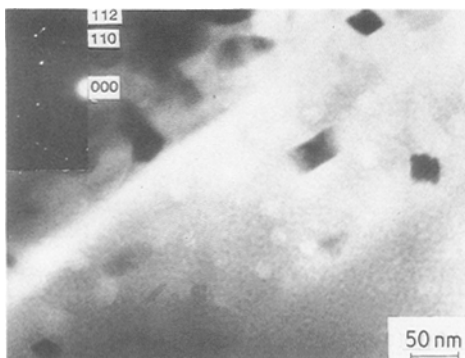


Figure 11 TEM micrograph of annealed deposit (870°C for 8 h) showing crystallization along the interface and inside the particle.

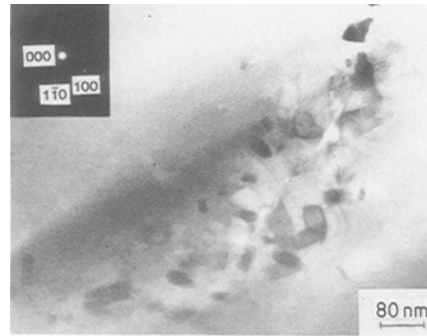


Figure 12 TEM micrograph of annealed deposit (870°C for 8 h) showing crystallization along a microcrack.

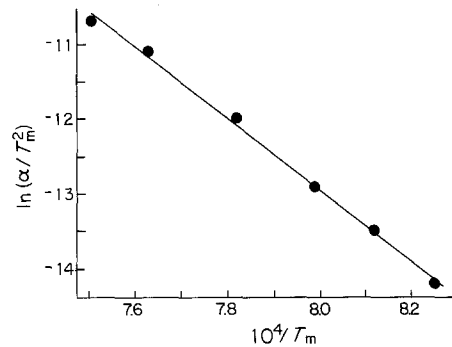


Figure 13 Kissinger plot for activation energy of phase transition from  $\mu$ -cordierite to high-cordierite.

( $57 \text{ kcal mol}^{-1}$ ), which is fairly close to the bulk cordierite enthalpy change of  $54 \text{ kcal mol}^{-1}$  [20].

#### 4. Conclusions

Sprayed cordierite is amorphous, undergoing an irreversible transformation to  $\mu$ -cordierite at about 800°C followed by another irreversible transformation to high-cordierite at ca. 1000°C. The transition temperature depends on the heating rate and sample size. The crystallization processes occur in amorphous material which had undergone decomposition into a modulated structure. The growth of  $\mu$ -cordierite from an amorphous phase at 870°C can be described by a Johnson-Mehl-Avrami-type Equation. The activation energy for crystal growth from the amorphous phase is  $1600 \text{ kJ mol}^{-1}$  and the activation energy of phase transition from  $\mu$ -cordierite to high-cordierite is  $400 \text{ kJ mol}^{-1}$ . The enthalpy change of the formation of high-cordierite is  $240 \text{ kJ mol}^{-1}$  for plasma-sprayed cordierite.

#### References

1. J. J. CLEVELAND, C. W. FRITSCH and R. N. KLEINER, in Proceedings of Gas Turbine Conference, American Society of Mechanical Engineers 1977, Paper no. 77-GT-98.
2. T. H. NIELSEN, *ibid.* Paper no. 77-GT-111.
3. Y. HIROSE, H. DOI and O. KAMIGAITO, *J. Mater. Sci. Lett.* 3 (1984) 95.
4. *Idem, ibid.* 3 (1984) 153.
5. R. GONZALEZ, Y. CHEN and K. L. TSANG, *J. Amer. Ceram. Soc.* 67 (1984) 775.

6. K. WATANABE and E. A. GIESS, *ibid.* **68** (1985) C-102.
7. H. S. KANOST, *Interceram* **28** (1967) 61.
8. I. M. LACHMAN, R. D. BAGLEY and R. M. LEWIS, *Amer. Ceram. Bull.* **60** (1981) 202.
9. M. D. KARKHANAVALA and F. A. HUMMEL, *J. Amer. Ceram. Soc.* **36** (1953) 389.
10. W. ZDANIEWSKI, *J. Mat. Sci.* **8** (1973) 192.
11. A. G. GREGORY and T. J. VEASEY, *ibid.* **6** (1971) 1312.
12. *Idem*, *ibid.* **8** (1973) 333.
13. W. ZDANIEWSKI, *J. Amer. Ceram. Soc.* **58** (1975) 163.
14. B. H. MUSSLER and M. W. SHAFER, *Amer. Ceram. Bull.* **63** (1984) 705.
15. M. E. FINE, "Introduction to Phase Transformation in Condensed System", (Macmillan, New York, 1964) Ch. 3.
16. C. M. JANTZEN and H. HERMAN, *J. Amer. Ceram. Soc.* **62** (1979) 212.
17. H. E. KISSINGER, *Anal. Chem.* **29** (1957) 1702.
18. K. MATUSITA, T. KOMATSU and R. YOKOTA, *J. Mat. Sci.* **19**(1984) 291.
19. H. G. WANG, H. HERMAN and X. LIU, "Activation Energy for Crystal Growth Using Iso-thermal and Continuous Processes", to be published.
20. A. NAVROTSKY and O. J. KLEPPA, *J. Amer. Ceram. Soc.* **56** (1973) 198.

*Received 17 December 1987  
and accepted 6 May 1988*